ELSEVIER

Journal of Power Sources 107 (2002) 48–55

JOURNAL OF POWER SOURCES

www.elsevier.com/locate/jpowsour

Study on the anode behavior of Sn and Sn–Cu alloy thin-film electrodes

Noriyuki Tamura*, Ryuji Ohshita, Masahisa Fujimoto, Shin Fujitani, Maruo Kamino, Ikuo Yonezu

New Materials Research Center, Sanyo Electric Co. Ltd., 1-18-13 Hashiridani, Hirakata, Osaka 573-8534, Japan

Received 19 March 2001; received in revised form 27 September 2001; accepted 18 October 2001

Abstract

Anodes based on tin metal powder offer large specific capacity, but also exhibit large irreversible capacity and poor cycle performance. In order to use them as a negative electrode for lithium secondary batteries, we focused on the electrodepositing process and investigated an electrodeposited tin layer on copper foil. In the full charge–discharge condition, charging and discharging between 0 and 2.0 V versus Li/Li^+, the first discharge capacity was 940 mAh g^{-1}, which was 2.5 times as large as that of graphite, and the coulomb efficiency in the first cycle was 93%, but its cycle performance was not improved.

In order to enhance the interface strength between the active material and the copper foil, we investigated an anode which was fabricated by annealing an as-deposited anode. In the full charge–discharge condition, the first charge–discharge characteristics were almost equivalent to the as-deposited anode, and the retention capacity ratio after 10 cycles was improved from 20 to 94%. It is considered that this improvement resulted from the formation of two different tin–copper intermetallic compound layers between the tin layer and the copper current collector due to the heat treatment.

A small cell using this annealed anode as a negative electrode was also investigated. This cell offered good cycle performance for the first 20 cycles.

Keywords: Tin; Electrodeposition; Interface strength; Annealing; Tin–copper alloys

1. Introduction

Many kinds of carbon materials are now widely used for the negative electrode of lithium ion batteries. As a result of our competitive development efforts, we were quick to find and improve a graphite with high crystallinity that offers approximately 370 mAh g^{-1} and good flatness in its voltage–capacity profile.

Recently, the demand for lithium ion batteries as a power supply for portable electric devices has steadily increased, and their capacity requirement has become larger. However, the capacity of graphite has already approached the theoretical limit of C_6Li (372 mAh g^{-1}). In order to enhance the energy density of lithium ion batteries, we have studied many anodic materials that offer larger specific capacity than graphite.

Tin-based materials have been focused on because their capacity (994 mAh g^{-1}, the theoretical limit of $Li_{4.4}Sn$) exceeds that of graphite [1–8]. Above all, tin oxides offer large capacity and good cycle performance, so that the energy density of lithium ion batteries is expected to rise by using them as a negative electrode [9–12]. However, one key issue for their commercialization remains unsolved. That is the large irreversible capacity caused by the reduction of the tin oxides and the formation of lithium oxide during the first cycle, as reported by Courtney and Dahn [3].

In order to reduce this irreversible capacity, we have studied several materials based on tin metal. First, a tin metal powder anode fabricated by slurry-coating on copper foil was investigated. Anodes with copper or carbon powder added as a conductive agent were also investigated [13]. The discharge capacity and the coulomb efficiency in the first cycle of the tin metal powder anode were 50 mAh g^{-1} and 9%, respectively. Adding conductive agents slightly enhanced those characteristics (e.g. Sn:C (1:1 wt.%) offered 280 mAh g^{-1}, 37%), but they were quite inferior to graphite. It is considered that the swelling of the tin metal particles during the first charge allowed them to fine and separate themselves from the other tin particles and the current collector [1], so that the electronic conductivity among the active material and at the interface between them and the current collector decreased in spite of adding the

* Corresponding author. Fax: +81-72-841-0302.
E-mail address: n_tamura@rd.sanyo.co.jp (N. Tamura).

0378-7753/02/$ – see front matter
PII: S0378-7753(01)00979-X

conductive agents, and the active material could not react with lithium after the first charge.

This result suggests that in order to use tin metal-based materials as a negative electrode for lithium secondary batteries, instead of the conventional electrode fabricated by slurry-coating onto a copper foil, where the slurry consists of active material, conductive agents and binders, a new type of electrode is needed, where the interface strength and electronic conductivity between the active material and the current collector is large, so that the active material can react with lithium stably. Accordingly, we focused on an electrodeposited electrode, whose interface strength is greater and whose cost is expected to be lower than conventional electrodes. In this paper, an electrodeposited tin layer on copper foil was therefore, investigated. To improve the electrodepositing process, an annealed type was also investigated.

2. Experimental

2.1. Preparation of an electrodeposited tin anode without/with heat treatment

An electrodeposited tin layer on electrolytic copper foil (foil thickness: 18 μm) was fabricated as shown in Fig. 1. After an acid-treatment for the copper foil, the tin layer was electrodeposited by using the bath described in Table 1 (anode: tin metal). The thickness of this tin layer was 2 μm. The size of the electrodeposited tin anode for the electrochemical charge–discharge test was 20 mm × 20 mm. The color of the active material was gray.

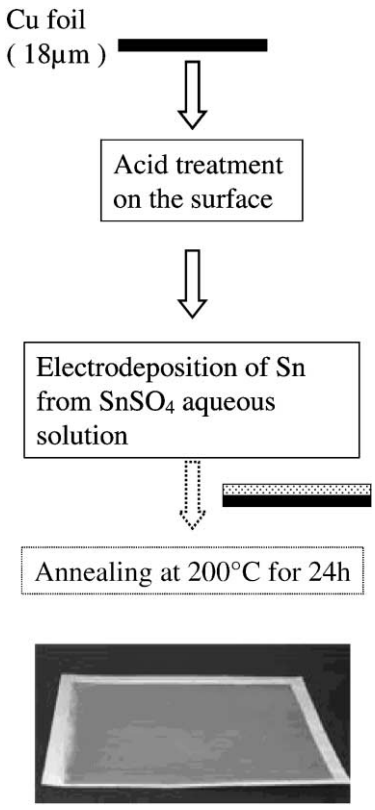

Fig. 1. Schematic flow of the preparation of the electrodeposited tin anode without/with heat treatment.

Table 1
Composition of the electrodeposition bath

Materials	Concentration
$SnSO_4$	40 g l^{-1}
H_2SO_4 (98%)	150 g l^{-1}
Formalin	5 cm^3 l^{-1}
Addition agent[a]	40 cm^3 l^{-1}

[a] Produced by Uyemura Kogyo Co. Ltd. Current density: 1 A cm^{-2}.

In order to investigate the effects of heat treatment, an electrodeposited tin anode with heat treatment was also fabricated by annealing the as-deposited anode at 200 °C for 24 h in vacuum. The color of the active material became slightly blackish from this heat treatment.

2.2. Electrochemical charge–discharge test

The electrochemical characteristics were measured using a three-electrode test cell. Lithium metal was employed as a counter electrode and a reference electrode. The electrolyte was EC/DMC = 1/1 containing 1 mol dm^{-3} $LiPF_6$. To remove water, the working electrode was annealed at 105 °C for 2.5 h before this test.

In order to use the full capacity of the active material, the test cell was charged (lithium intercalation) to 0 V versus Li/Li^+ at three successive steps of decreasing current density, 0.25, 0.13, and 0.05 mA cm^{-2}, and was discharged to 2 V versus Li/Li^+ at the same steps of current density. In previous reports [1,4,5], limiting the range of the charge–discharge potential improved the cycle performance of electrodeposited tin-based anodes. Nevertheless, we selected these test conditions because our requirement for anode materials is that they have at least twice the capacity of graphite and good cycle performance at the same time under practical conditions where the range of the charge–discharge potential is limited by the active materials.

The weight of the active material in the investigated anodes was measured by analyzing the amount of tin contained in them by ICP spectrometry.

2.3. Structural analysis

The structures of the active materials in the electrodeposited anodes without/with heat treatment were investigated by backscattered electron images (BEI; Hitachi S-4500) and analyzed by X-ray diffractometry (XRD; Rigaku Rotaflex, Cu Kα, 40 kV–100 mA). Electrodes were buried in resin and polished to take the BEI of their cross-sections. The test pieces for XRD were fabricated by putting the anodes onto a glass plate.

In order to analyze the composition of the active materials of these anodes in greater detail, they were also analyzed by an X-ray microanalyzer (XMA; Kevex, Sigma, energy dispersion type), which shows their composition ratio.

2.4. Preparation of a small cell

A small cell using this annealed anode (thickness: 2 μm) as a negative electrode was fabricated. The cell consisted of one stack of $LiCoO_2$/separator/this annealed anode. The size of the positive electrode was 20 mm × 20 mm, and that of the negative electrode was 25 mm × 25 mm. The electrolyte was EC/DEC = 1/1 containing 1 mol dm^{-3} $LiPF_6$. These were set in an Al-laminated package, whose size was 35 mm × 50 mm × 0.4 mm. This small cell was charged for 6 mAh at a constant current density of 1.2 mA and was discharged to 2.25 V at the same current density.

3. Results and discussion

3.1. Charge–discharge characteristics of the electrodeposited tin anode without heat treatment

The charge–discharge curves of the electrodeposited tin anode without heat treatment in the first cycle are shown in Fig. 2. For comparison, the curves of the tin metal powder anode (particle size: under 250 mesh; binder: PVdF) and a standard graphite anode fabricated by slurry-coating on copper foil are also shown. In charging, the potential of the electrodeposited anode changed to 0.4 V versus Li/Li^+ immediately after starting the test, stabilized, and then gradually changed toward the negative again. It is considered that the plateau resulted from the reaction of LiSn with lithium [1], and that the gradual increase resulted from a coexistence with several Sn–Li alloy phases in the active material due to the large current density. In discharging,

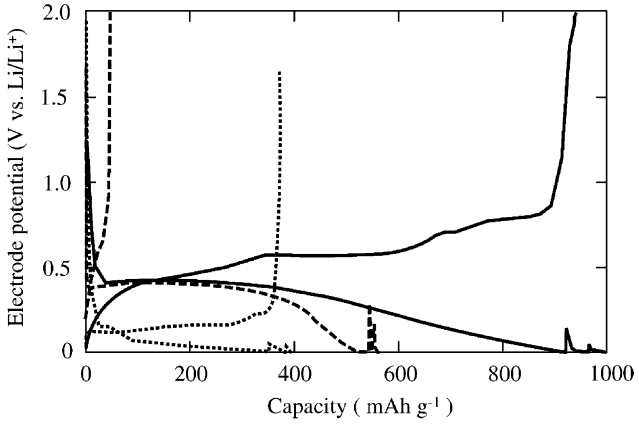

Fig. 2. Initial charge–discharge curves of several anodes. Electrode potential range: 0–2 V vs. Li/Li^+, charge–discharge current density: 0.25–0.13–0.05 mA cm^{-2}; solid line, electrodeposited tin; dashed line, tin metal powder; dotted line, graphite.

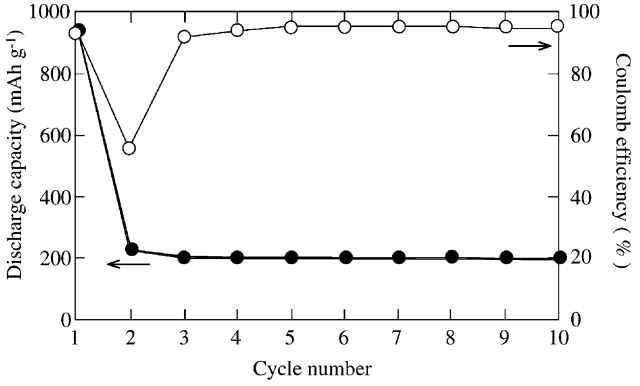

Fig. 3. Cycle performance of the electrodeposited anode. Electrode potential range: 0–2 V vs. Li/Li^+, charge–discharge current density: 0.25–0.13–0.05 mA cm^{-2}.

more plateaus were clearly observed. Note that the discharge curve of the electrodeposited anode in Fig. 2 shows a result only at 0.25 mA cm^{-2}. The discharge capacity at the following current density steps, 0.13 and 0.05 mA cm^{-2}, was almost zero during the first 10 cycles.

The first charge capacity of 940 mAh g^{-1} was close to the theoretical limit (994 mAh g^{-1}), and was 2.5 times as large as that of graphite. The coulomb efficiency in the first cycle was 93%, which was almost equal to that of graphite. This suggests that the anode fabricated by this electrodepositing process benefits from improved electronic conductivity among its active material and/or at the interface between them and the current collector, in comparison with the tin metal powder anode fabricated by the conventional slurry-coating process, and that the charge–discharge characteristics in the first cycle improved to a level approaching graphite.

Fig. 3 shows the cycle performance of the discharge capacity and coulomb efficiency of the electrodeposited tin anode without heat treatment. Although the discharge capacity in the first cycle was 940 mAh g^{-1}, it decreased to almost 200 mAh g^{-1} in the second, and never recovered in the following cycles. A significantly low cycle performance in the second cycle is observed. In the following cycle, the coulomb efficiency was over 90%, and did not decrease further.

These results indicate that the electrodepositing process without heat treatment can improve the charge–discharge characteristics in the first cycle, but offer no significant improvement to the cycle performance. It is assumed that this results from a lack of interface strength between the entire part of active material and the current collector.

3.2. Charge–discharge characteristics of the electrodeposited tin anode with heat treatment

In order to improve the interface strength between the active material and the current collector, an electrodeposited tin anode with heat treatment was investigated. The charge–discharge curves in the first cycle are shown in Fig. 4. In

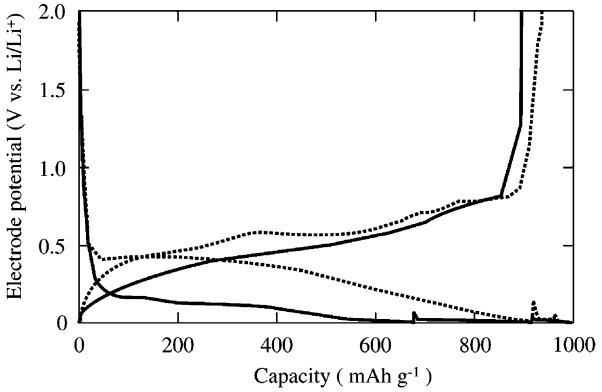

Fig. 4. Initial charge–discharge curves of the electrodeposited anodes. Electrode potential range: 0–2 V vs. Li/Li^+, charge–discharge current density: 0.25–0.13–0.05 mA cm^{-2}; solid line, annealed at 200 °C for 24 h; dotted line, as-deposited.

comparison with the as-deposited anode, the potential of the annealed anode shifted to negative during the first cycle, and changed more gradually. This suggests that tin (the active material) and copper (the current collector) were alloyed by the heat treatment, as discussed here. Note that the discharge curve of this anode shows a result only at 0.25 mA cm^{-2} in Fig. 4. The discharge capacity at the following current density steps, 0.13 and 0.05 mA cm^{-2}, was nearly zero during the first 10 cycles, like the as-deposited anode.

The first discharge capacity was 905 mAh g^{-1}, which was almost equal to that of the as-deposited anode, and the coulomb efficiency in the first cycle was 90%. This result indicates that the first charge–discharge characteristics of the annealed anode were equivalent to those of the as-deposited one.

Fig. 5 shows the cycle performance of the discharge capacity and coulomb efficiency of the annealed anode, respectively. The charge capacity and coulomb efficiency in the second cycle were significantly improved, and the retention capacity ratio after the first 10 cycles was improved from 20 to 94%.

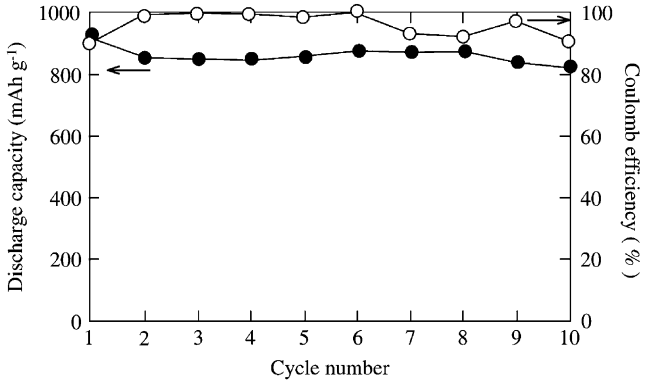

Fig. 5. Cycle performance of the electrodeposited anodes. Electrode potential range: 0–2 V vs. Li/Li^+, charge–discharge current density: 0.25–0.13–0.05 mA cm^{-2}.

This result indicates that the heat treatment process can improve the cycle performance of an electrodeposited tin anode. It is assumed that this is because the interface strength between the entire part of the active material and the current collector is enhanced by this heat treatment, so that the former can be active during the first 10 cycles.

3.3. Heat treatment effects on the structures of the active materials

The differences in the structures of the active materials before and after heat treatment were observed by BEI, XMA, and XRD.

Fig. 6 shows a cross-section of the as-deposited and annealed anodes. In the as-deposited anode, there were two layers, an active material layer and a current collector, and the color of the former was uniformly white, which indicates that almost the entire part of the active material consisted of pure tin. In the annealed anode, by contrast, three layers of active material were formed on the current collector, and the thickness of the part of the active material increased. The colors of the layers changed stepwise from dark to light gray from the current collector to the surface, those of the no. 1 and 2 layers were the same, and the color of each layer was uniform throughout the layer. These results suggest that tin and copper diffused into each other's layer, and formed two different Sn–Cu alloys, which contained a uniform composition of tin and copper throughout each layer. They also suggest that the copper concentration of each layer decreased stepwise from the current collector to the no. 1 layer.

It was further observed that there were nano-order pores in the no. 1 layer. The thickness of this layer was about 2 μm. It is considered that these pores were formed from the burning of organic impurities in the tin layer of the as-deposited anode, and that the current collector layer had been under those pores before heat treatment. Note that some large pores with a size of about 0.5 μm were observed not only in the annealed anode but also in the as-deposited anode. It is considered that these pores resulted from the electrodepositing conditions, e.g. the lack of acid treatment before electrodeposition.

According to XMA data, the active material layer in the as-deposited anode consisted of 100% Sn, and the layers in the annealed anode consisted of Cu:Sn = 6:4 phase (no. 1 and 2 layers), and Cu:Sn = 8:2 phase (no. 3 layer). In addition to these layers, there was a 100% Sn thin layer (<500 nm) on the surface of the annealed anode. These results clearly indicate that the copper concentration of each layer of the annealed anode decreased stepwise from the current collector to the no. 1 (no. 2) layer.

Fig. 7 shows the XRD patterns of the as-deposited and annealed anodes. A Cu_6Sn_5 phase is observed in addition to tin and copper in the as-deposited anode. This result indicates that the electrodeposition process without heat treatment formed a slight Sn–Cu intermetallic compound, which probably existed at the interface between tin and copper. Fig. 7 also shows that there was an Sn–Cu alloy phase like

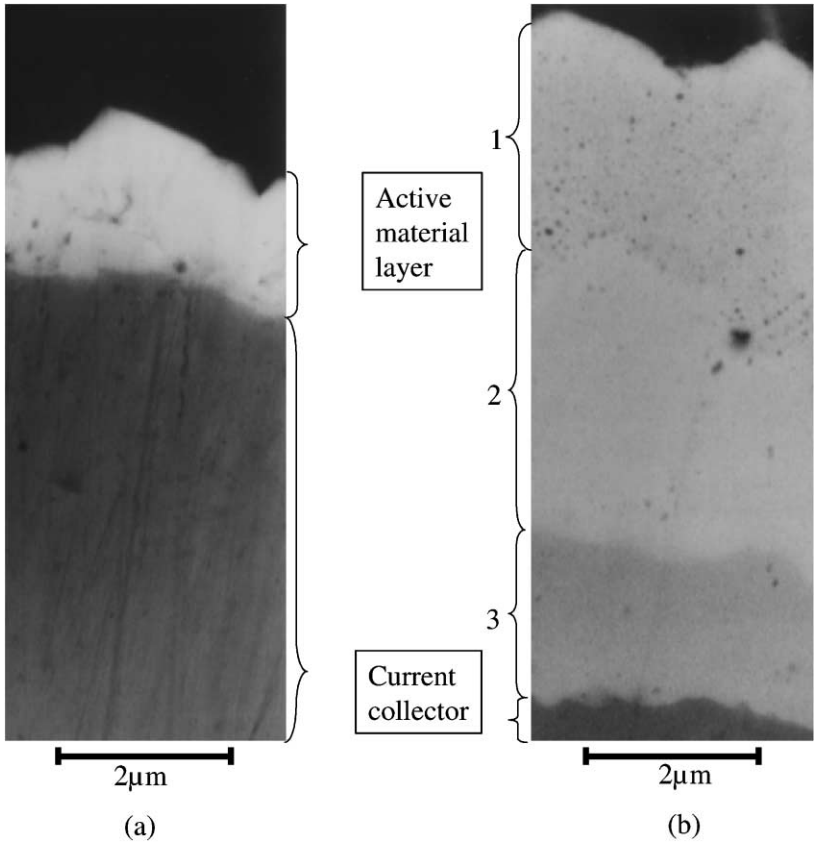

Fig. 6. Microstructures of (a) the as-deposited and (b) the annealed anodes (13,000×).

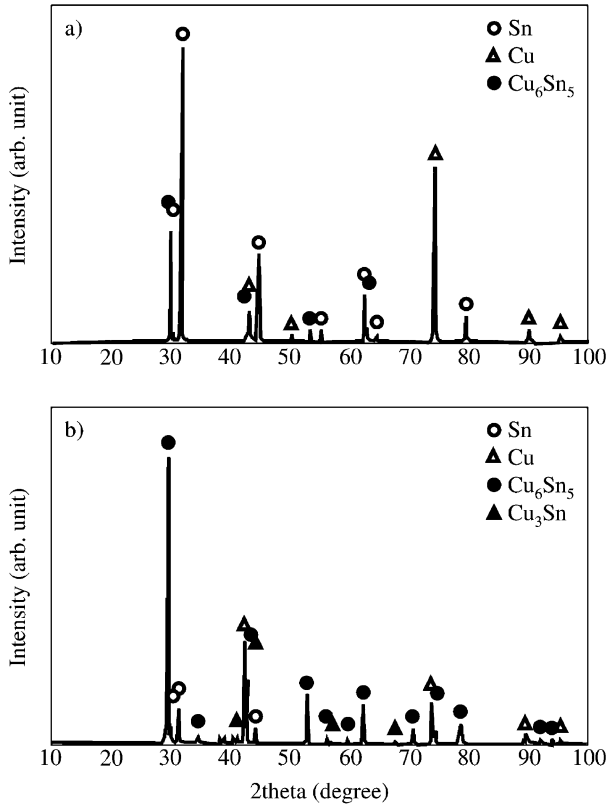

Fig. 7. XRD patterns of (a) the as-deposited and (b) the annealed anodes.

Cu_3Sn in addition to tin, Cu_6Sn_5, and copper in the annealed anode. Comparing this with XMA data, it is considered that the Cu:Sn = 6:4 phase and Cu:Sn = 8:2 phase correspond to the Cu_6Sn_5 and Cu_3Sn-like phase, respectively. Fig. 8 shows schematic models of the structures of these anodes. Note that Fig. 7 shows the tin oriented to [1 0 1], which resulted from the electrodeposition process. This probably affected both the alloying and the cycle performance.

3.4. Heat treatment effects on cycle performance

The relation between the structures of the active materials and the cycle performance of the as-deposited and annealed

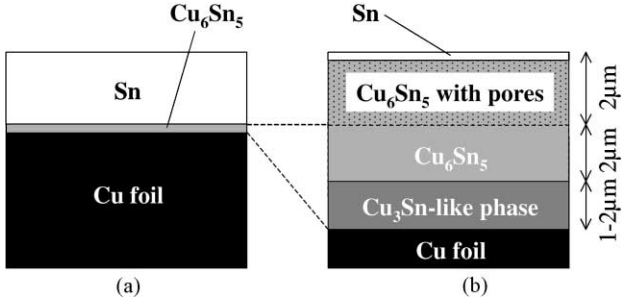

Fig. 8. Schematic models of the microstructures of (a) the as-deposited and (b) the annealed anodes. The thickness of both Cu_6Sn_5 in the as-deposited anode and surface Sn on the annealed anode are <0.5 μm.

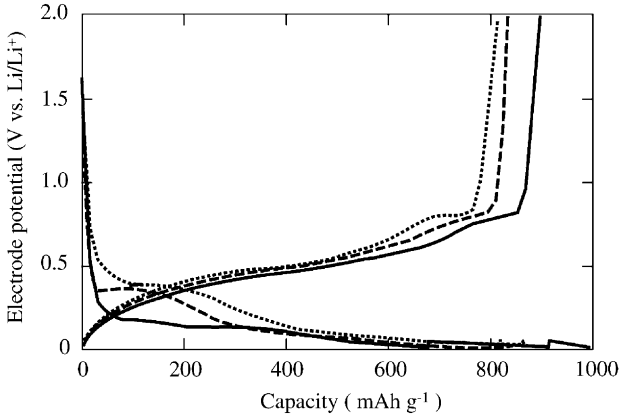

Fig. 9. Charge–discharge curves of the annealed anode in various cycles. Electrode potential range: 0–2 V vs. Li/Li^+, charge–discharge current density: 0.25–0.13–0.05 mA cm^{-2}; solid line, first cycle; dashed line, second cycle; dotted line, tenth cycle.

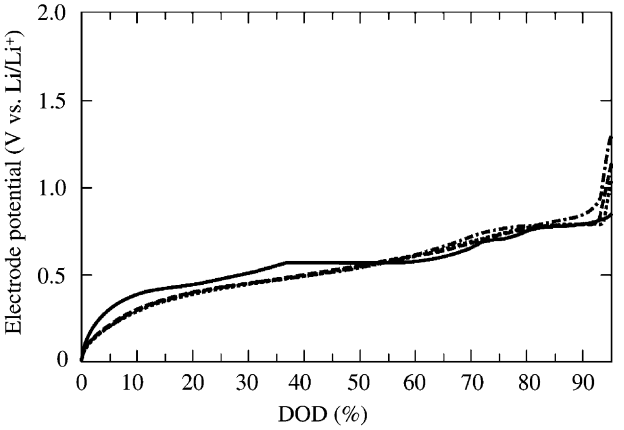

Fig. 11. Discharge curves of the as-deposited anode in various cycles. Electrode potential range: 0–2 V vs. Li/Li^+, discharge current density: 0.25–0.13–0.05 mA cm^{-2}; solid line, first cycle; dashed line, second cycle; dotted line, third cycle; dashed dotted line, tenth cycle.

anodes were investigated by considering their charge–discharge curves.

Fig. 9 shows the charge–discharge curves of the annealed anode in the first, second, and tenth cycles. Compared with those of Cu_6Sn_5 [14,15], the potential of this anode shifted to negative and its profile showed a different shape in the first cycle. However, in the following cycle, both the potential and profile resembled those of Cu_6Sn_5. In the annealed anode, therefore, it is considered that although Sn, Cu_6Sn_5, and Cu_3Sn-like phases reacted with lithium in the first charge, only Cu_6Sn_5 was the main reactant in the first discharge and following cycles, and the potential changed a little more gradually than that of Cu_6Sn_5 because of the competitive reaction of the residual active tin with lithium.

Figs. 10 and 11 show the charge and discharge curves of the as-deposited anode in the first, second, third and tenth cycles, respectively. In the second discharge and the following cycle, both the potential and profile resembled those of Cu_6Sn_5. This result indicates that the same active material as that of the main reactant of the annealed anode, which formed slightly at the interface between tin and the current collector by the electrodeposition process without heat treatment, was the main reactant after the second charge, so that the retention capacity ratio did not decrease further. Moreover, this part of the active material was thin and close to the current collector, enabling it to be active in the following cycle. Fig. 10 also shows a plateau at 1.5 V versus Li/Li^+ only in the second charge. Considering the large capacity of this plateau (140 mAh g^{-1} = 35% SOC), and also considering the fact that it was not observed in the first charge and that it has been observed in other reports [3,16], it may be attributed to the reduction of electrolytes on the catalytic sites of the active Sn surface rather than to the reduction of contaminants in the Sn layer. Assuming that this plateau is not related to a reaction of lithium with the active material, the real coulomb efficiency in the second cycle is 85%. This suggests that the significantly low cycle performance of the as-deposited anode in the second cycle mainly resulted from an increase in the amount of inactive material. During the first discharge, it is considered that a main part of the active material (100% tin) becomes inert as a result of separation from another part that is electrically connected with the current collector, and that the other part becomes finer but maintains the electronic connection with the current collector, thus, increasing the catalytic sites of their surfaces.

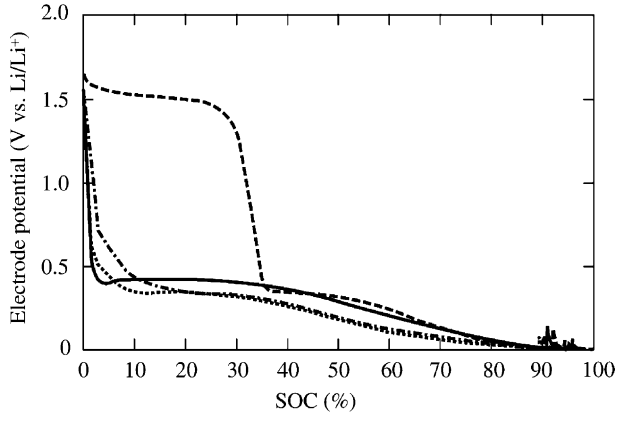

Fig. 10. Charge curves of the as-deposited anode in various cycles. Electrode potential range: 0–2 V vs. Li/Li^+, charge current density: 0.25–0.13–0.05 mA cm^{-2}; solid line, first cycle; dashed line, second cycle; dotted line, third cycle; dashed dotted line, tenth cycle.

These results suggest the following mechanism of cycle performance improvement by heat treatment: first, tin and copper diffuse into each other's layer by heat treatment, and form two different Sn–Cu intermetallic compound layers between the surface tin layer and the copper current collector. In the Sn–Cu intermetallic compound layer, compared with the tin layer, the existence of lithium-inert copper decreases the amount of swelling of the active material during the reaction with lithium. It is considered that this also decreases the reactivity of the active material with the

electrolytes at the same time. Among the layers of the active material, the tin concentration of each layer increases from the current collector to the surface, so that the difference in the amount of swelling of the active material between the adjacent layers becomes smaller than before heat treatment, the stress on the interfaces between the layers by the swelling of the active material decreases, and the separation of the active material from the interface of each layer is suppressed. These heat treatment effects control the fining of the entire active material, its reaction with the electrolytes, and the decrease of the electronic conductivity among the active material and between themselves and the current collector, so that the cycle performance is improved.

3.5. The charge–discharge characteristics of a small cell using the electrodeposited tin anode with heat treatment as a negative electrode

In order to study the charge–discharge characteristics and long cycle performance of the electrodeposited tin anode used as a negative electrode for a lithium ion battery, a small cell using the annealed anode (positive electrode: $LiCoO_2$) was fabricated and investigated. The charge–discharge curve of this cell in the first cycle is shown in Fig. 12. The average discharge voltage was 3.27 V, which is slightly lower than that of a cell using graphite as a negative electrode. This cell showed good flatness in its voltage–capacity profile.

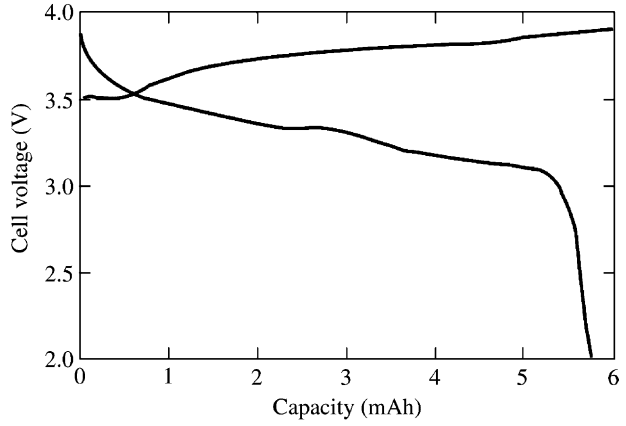

Fig. 12. Initial charge–discharge curves of the small cell using the annealed anode as a negative electrode. Charged for 6 mAh at 1.2 mA and discharged to 2.25 V at 1.2 mA.

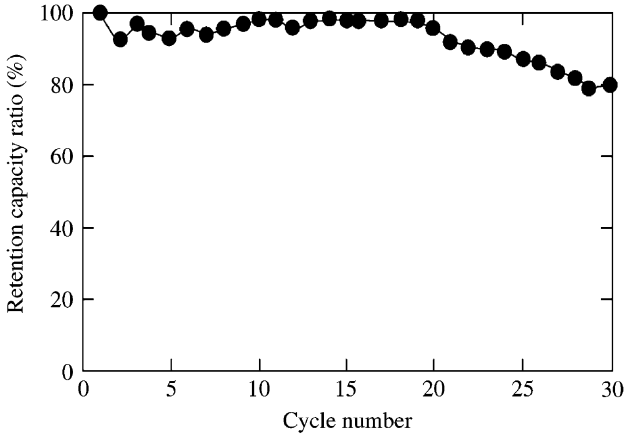

Fig. 13. Cycle performance of the small cell using the annealed anode as a negative electrode. Charged for 6 mAh at 1.2 mA and discharged to 2.25 V at 1.2 mA.

The cycle performance of this cell, as shown in Fig. 13, was good in the first 20 cycles, but gradually deteriorated in the following cycles.

4. Conclusion

In order to use tin metal as a negative electrode for lithium secondary batteries with large energy density, we focused on a new type of electrode fabricated by an electrodepositing process, which enhances the interface strength and electronic conductivity between the active material and the current collector and leads to a stable reaction of the active material with lithium, and investigated an electrodeposited tin layer on copper foil. In the full charge–discharge condition, charging and discharging between 0 and 2.0 V versus Li/Li^+, the first discharge capacity was 940 mAh g^{-1}, which was 2.5 times as large as that of graphite, and the coulomb efficiency in the first cycle was 93%, but its cycle performance was poor. It is considered that this resulted from a lack of interface strength between the entire part of the active material and the current collector in spite of the formation of a small amount of Cu_6Sn_5 due to the electrodeposition.

In order to enhance the interface strength between the active material and the copper foil, we investigated an anode fabricated by annealing an as-deposited anode. In the full charge–discharge condition, the first charge–discharge characteristics were almost equivalent to those of the as-deposited anode, and the retention capacity ratio after 10 cycles was improved from 20 to 94%. This annealing induced the formation of two different Sn–Cu intermetallic compound layers between the tin layer and the copper current collector. It is considered that introducing copper in the tin phase and its concentration gradient enhanced the interface strength between the active material and the current collector, and thus, the cycle performance was improved.

A small cell using this annealed anode as a negative electrode (positive electrode: $LiCoO_2$) was also investigated. This cell showed good flatness in its voltage–capacity profile. The cycle performance was good in the first 20 cycles, but gradually deteriorated in the following cycles.

References

[1] M. Winter, J.O. Besenhard, Electrochim. Acta 45 (1999) 31–50.
[2] R.A. Huggins, J. Power Sources 81/82 (1999) 13–19.
[3] I.A. Courtney, J.R. Dahn, J. Electrochem. Soc. 144 (1997) 2045–2052.

[4] J. Yang, M. Winter, J.O. Besenhard, Solid State Ionics 90 (1996) 281–287.
[5] J.O. Besenhard, J. Yang, M. Winter, J. Power Sources 68 (1997) 87–90.
[6] A.H. Whitehead, J.M. Elliott, J.R. Owen, J. Power Sources 81/82 (1999) 33–38.
[7] J. Yang, Y. Takeda, N. Imanishi, O. Yamamoto, J. Electrochem. Soc. 146 (1999) 4009–4013.
[8] G.M. Ehrlich, C. Durand, X. Chen, T.A. Hugener, F. Spiess, S.L. Suib, J. Electrochem. Soc. 147 (2000) 886–891.
[9] Y. Idota, T. Kubota, A. Matsufuji, Y. Maekawa, T. Miyasaka, Science 276 (1997) 1395–1397.
[10] M. Nagayama, T. Morita, H. Ikuta, M. Wakihara, M. Takano, S. Kawasaki, Solid State Ionics 106 (1998) 33–38.
[11] R. Retoux, T. Brousse, D.M. Schleich, J. Electrochem. Soc. 146 (1999) 2472–2476.
[12] H. Morimoto, M. Nakai, M. Tatsumisago, T. Minami, J. Electrochem. Soc. 146 (1999) 3970–3973.
[13] N. Tamura, R. Ohshita, M. Fujimoto, S. Fujitani, M. Kamino, I. Yonezu, in: Proceedings of the 41st Battery Symposium in Japan, Nagoya, 2000, p. 540.
[14] K.D. Kepler, J.T. Vaughey, M.M. Thackeray, Electrochem. Solid-State Lett. 2 (1999) 307–309.
[15] D. Larcher, L.Y. Beaulieu, D.D. MacNeil, J.R. Dahn, J. Electrochem. Soc. 147 (2000) 1658–1662.
[16] S. Beattie, J.R. Dahn, in: Proceedings of the 2001 Joint International Meeting, San Francisco, 2001, p. 275.